

Density functional theory screened-exchange approach for investigating electronic properties of graphene-related materials

Roland Gillen* and John Robertson

Department of Engineering, University of Cambridge, Cambridge CB3 0FA, United Kingdom

(Received 17 June 2010; published 3 September 2010)

We present *ab initio* calculations of the band structure of graphene and of short zigzag graphene nanoribbons (ZGNRs) by the screened-exchange-local-density approximation (LDA) method within the framework of density functional theory. The inclusion of nonlocal electron-electron interactions in this approach results in a renormalization of the electronic band structure and the Fermi velocity compared to calculations within LDA gives good agreement with experiment. Similarly, the band gaps in ZGNRs are widened by more than 200%, being of similar magnitude than band gaps from past studies based on quasiparticle band structures. We found a noticeable effect of nonlocal exchange on the spin polarization of the electronic ground state of ZGNRs, compared to LDA and generalized gradient approximation calculations.

DOI: [10.1103/PhysRevB.82.125406](https://doi.org/10.1103/PhysRevB.82.125406)

PACS number(s): 31.15.E-, 81.05.ue, 73.22.Pr

I. INTRODUCTION

Since the first successful preparation of free-standing graphene, an isolated layer of graphite, in 2004,¹ a considerable amount of both theoretical and experimental work have been employed on investigations of its unique physical properties. Graphene is a zero-gap semiconductor where the π valence band and the π^* conduction band contact at the six Dirac points in the hexagonal graphene Brillouin zone. A peculiar property of graphene is the linear dispersion $E = \hbar v_F |\vec{k}|$ (v_F is the Fermi velocity) of the π bands near the K points, resulting in effectively massless Dirac fermions.² This property, predicted theoretically and confirmed experimentally, is appealing for theoretical scientists, as it allows, in principle, to study relativistic Dirac fermions by methods from condensed-matter physics. Similarly, the outstanding electronic properties turn graphene and its related materials, such as carbon nanotubes and graphene nanoribbons, to promising materials for application in nanoelectronics. For this reason, a thorough understanding of the electronic properties of graphene materials is significant.

A common and efficient method for the study of ground-state properties in condensed-matter physics are *ab initio* density functional theory calculations within the local-density approximation (LDA) or generalized gradient approximation (GGA). Whereas those approaches, in all their simplicity, usually yield good results for structural properties they routinely underestimate electronic properties, e.g., band gaps. Recent reports of experimental studies of charge carrier dynamics in graphene by use of angle-resolved photoemission spectroscopy (ARPES),^{3,4} IR measurements,⁵ magnetotransport measurements,⁶ scanning tunneling microscopy (STM),⁷ and cyclotron resonance scans,⁸ revealed that common density functional theory calculations severely underestimate the Fermi velocity by 15–20%. This was attributed to prominent many-body effects in graphene such as nonlocal electron-electron and electron-phonon interaction, which are not accounted for in the LDA framework and lead to a renormalization of the Fermi velocity. Similarly, calculations within LDA underestimate the band-gap sizes in both armchair and zigzag graphene nanoribbons (ZGNRs) (Ref. 9) by 50–75%, bad performances even for LDA calculations

on semiconductors. Several authors have reported that self-energy corrections of the LDA band structures using many-body G_0W_0 approximations can amend the shortcomings of LDA. For the Fermi velocity, those corrections yield values that are in good agreement with experimental results.^{10–13} However, while quasiparticle corrections produce accurate results, the considerable computational effort here is an undeniable disadvantage.

There are several attempts to improve on the shortcomings of LDA by including nonlocal expressions directly in the exchange-correlation functional. In case of the screened-exchange-LDA (sX-LDA) approximation, the electron-correlation functional is modeled by a blend of LDA and a statically screened Hartree-Fock exact exchange potential in order to account for electron-electron interactions to some extent but retaining the advantages of LDA.^{14–16} An obvious advantage of this method is the lowered computational costs compared to GW, which permits self-consistent solution of the Kohn-Sham equations within sX-LDA and the calculations of total energy and charge and spin densities. Further, it has been shown that the screened-exchange method indeed is successful in describing the band gaps of various materials with accuracy comparable to G_0W_0 .^{17,18}

Motivated by that success, we want to use this paper to report calculations on the band structure of graphene and zigzag graphene nanoribbons employing sX-LDA. We found that the calculated renormalization of the Fermi velocity in graphene due to electron-electron interactions compares well with experimental values and the ones from quasiparticle corrections.^{10–13} Further, we show that the nonlocal exchange has a considerable effect on the spin polarization and the electronic band structures of zigzag nanoribbons, which again compare well with quasiparticle band structures.¹⁹

II. METHOD

Our study of the electronic band structures of graphene and zigzag graphene nanoribbons is based on pseudopotential density functional theory in the framework of the screened-exchange-LDA approximation, LDA and GGA in the Perdew-Wang description from 1991 (PW91), and was performed by use of the computational package CASTEP.²⁰

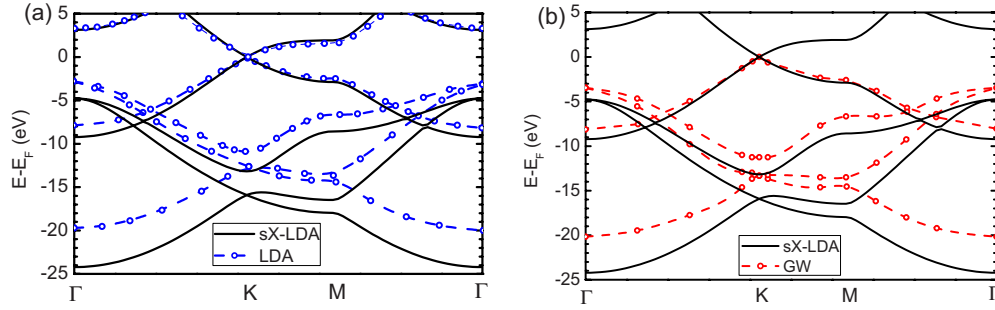


FIG. 1. (Color online) Comparison of the band structure of graphene within the screened-exchange approximation with (a) the band structure within the LDA and (b) the quasiparticle band structure from self-energy corrections within the G_0W_0 approximation, which was extracted from Ref. 11.

Graphene was modeled by the common two-atomic Wigner-Seitz unit cell and periodic boundary conditions in the three spatial directions. We found that a distance of 9.6 Å between the periodic images is sufficient to minimize interlayer interactions and represent graphene as a two-dimensional crystal. The action of the atomic core were described by standard norm-conserving pseudopotentials,²¹ the valence electrons by plane waves with a cutoff energy of 750 eV. Integrations in the reciprocal space were done by a Monkhorst-Pack grid²² of $9 \times 9 \times 1$ equidistant points in the Brillouin zone of graphene. We further optimized the atomic positions until the maximum interatomic force were lower than 0.001 eV/Å. We modeled graphene nanoribbons by a rectangular unit cell being continued periodically along the nanoribbon axis and used an energy cutoff of 750 eV and a k -point grid of $1 \times 1 \times 9$ points along the Brillouin zone. The cell dimensions were chosen in a way to minimize interlayer interaction between the periodic images and to maintain the calculational effort at the same time. As for graphene, we found that a distance of 9.6 Å between periodic images is a sufficient compromise. The dangling bonds of the carbon atoms at the nanoribbons edges were passivated with hydrogen atoms in order to maintain the sp^2 hybridization. The geometries of all nanoribbons were fully optimized.

III. RESULTS AND DISCUSSION

A. Band structure of graphene

We used these parameters to calculate the electronic band structures of graphene using LDA, GGA, and sX-LDA.

Figure 1(a) compares the valence bands of graphene from calculations within the local-density approximation and with screened exchange. There is a visible renormalization of the band structure due to the inclusion of nonlocal correlation effects. Screened exchange results in a general shift of the three valence σ bands to lower energies and that is most significant near the Γ point. There, the two degenerate bands from sX-LDA have energies of -5 eV compared to -3.3 eV from LDA. The conduction bands are not affected as much from nonlocal exchange. This might correlate with studies by Lee *et al.*,²³ who argue that the improved band gaps from screened-exchange-LDA functionals in the materials they studied mainly originate from a marked downshift of the valence bands. This lowered energy of the valence bands

compared to the Fermi energy results in a broadened band gap by 1.7 eV at the Γ point. The π bands from both calculated band structures coincide fairly well in the K-M part of the Brillouin zone. In the Γ -K and Γ -M parts of the band structure, the nonlocal electron interaction results in a visibly increased slope for the sX-LDA π band in respect to the π band from LDA. This results in a renormalized Fermi velocity,

$$v_F = \frac{1}{\hbar} \frac{\partial E}{\partial k} \quad (1)$$

in the linear part of the π bands from sX-LDA compared to LDA. The Fermi velocity is a particularly interesting variable in semiconductors and conductors, as it is comparable to the velocity of the electrons that contribute to electric conduction. Table I shows a number of recently reported experimental values for the Fermi velocity, which are between 1.0×10^6 and 1.1×10^6 m/s. For the band structure from LDA, we found a Fermi velocity of 8.9×10^5 m/s, which underestimates the reported experimental Fermi velocities by 11–19% (depending on the experiment). Calculations within the generalized gradient approximation yield the same result, see Table I. In contrast, the steeper slope in the sX-LDA band structure results in a Fermi velocity of 1.16×10^6 m/s, being in good agreement with the values from magnetotransport⁷ and STM (Ref. 6) measurements.

TABLE I. *Ab initio* and experimental values of the Fermi velocity in the linear valence bands of graphene.

Method	Fermi velocity v_F (m/s)
LDA	0.89×10^6
GGA	0.88×10^6
sX-LDA	1.16×10^6
G_0W_0 (CD integration) (Ref. 11)	1.12×10^6
G_0W_0 (RPA+PP) (Ref. 12)	1.25×10^6
Experiment (ARPES) (Ref. 4)	$1.0 \pm 0.05 \times 10^6$
Experiment (IR) (Ref. 5)	$1.02 \pm 0.01 \times 10^6$
Experiment (magnetotransport) (Ref. 7)	$1.07 \pm 0.01 \times 10^6$
Experiment (STM) (Ref. 6)	1.1×10^6
Experiment (cyclotron) (Ref. 8)	1.093×10^6

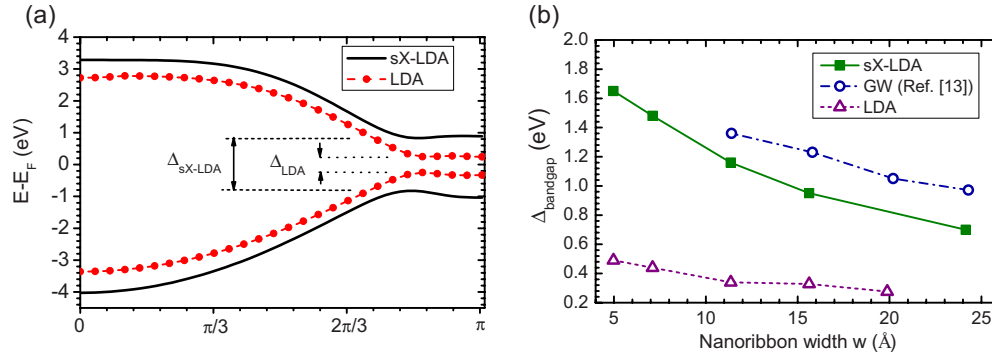


FIG. 2. (Color online) (a) Edge bands of a small zigzag nanoribbon (six carbon atoms) from calculations employing screened-exchange (solid lines) and local-density approximation (filled dots and broken lines). (b) Comparison of the band-gap sizes of zigzag nanoribbons of various widths from sX-LDA (circles), LDA+ G_0W_0 (squares), and LDA (triangles) calculations. The G_0W_0 results were taken from Ref. 19.

Figure 1(b) shows the valence bands from calculations within sX-LDA, together with quasiparticle energies at selected k points from G_0W_0 calculations by Trevisanutto *et al.*¹¹ The G_0W_0 calculations build upon LDA wave functions and have been performed by use of a contour-deformation (CD) integration, which is known to provide the most accurate results in G_0W_0 quasiparticle corrections. As with sX-LDA, the correlation effects induce a shift of the three σ bands to lower energies but the downshift is considerably weaker and of magnitude < 1 eV. Unfortunately, the authors did not report any data for the conduction-band energies. Lee *et al.*,²³ however, found that the improved band gaps from G_0W_0 result from a strong upshift of the conduction bands. The π band from sX-LDA shows a very good agreement with the π band in the quasiparticle band structure, except for deviations near the Γ point. The value of the Fermi velocity was reported to be 1.12×10^6 m/s, i.e., only slightly closer to experimental values than our result. This encourages us to believe that the electronic properties of graphene and graphene-based materials can be described in good accuracy within the framework of the screened-exchange approximation.

B. Spin-induced band gaps in zigzag nanoribbons

The first investigations of the electronic structures of graphene nanoribbons were based on simple zone-folding arguments, neglecting effects from the nanoribbon edges. In this approximation, one third of all nanoribbons with armchair edges and all zigzag nanoribbons should be metallic or zero-gap semiconductors,^{24,25} similar to the situation in carbon nanotubes. More elaborate investigations employing density functional theory predicted that the existence of a large ratio of edge to “bulk” atoms in carbon nanoribbons indeed has a prominent effect on the electronic structure. For zigzag nanoribbons, the deciding factor is edge-localized electron states, which possess a large density of states at the Fermi energy. Using a Hubbard model, Fujita *et al.*²⁴ showed that the resulting Fermi instability leads to the formation of an antiferromagnetic ground state in monohydrogenated nanoribbons in contrast to the dielectric graphene. This spin-polarized ground state involves the opening of a direct band

gap as the system wants to lower the density of states near the Fermi level and remove the instability.²⁶

Investigations employing LDA predict that the band-gap size is lower than 0.5 eV for all zigzag nanoribbons and scales antiproportionally with the nanoribbon width due to the decrease in spin interaction between the atoms at opposite edges.⁹ It might be expected from this interaction that nonlocal components of the electron exchange are of importance for the band-gap size and that LDA, neglecting nonlocal exchange, is not sufficient to fully describe the electronic properties of zigzag nanoribbons. Indeed, our calculations exhibit marked changes in the band-gap size due to the inclusion of nonlocal exchange. Figure 2(a) shows the electron bands of the edge states of a small zigzag nanoribbon from LDA and sX-LDA calculations. While both band structures qualitatively exhibit similar dispersion, the band gap near $k = \frac{2\pi}{a}$ is widened by more than 200% from a value of 0.5 eV in LDA to 1.65 eV in sX-LDA. Our calculated band-gap energies are comparable to those obtained from G_0W_0 quasiparticle corrections on LDA wave functions by Yang *et al.*,¹⁹ see Fig. 2(b), but the quasiparticle band gaps are consistently 0.2 eV larger than our values. Another study, employing the B3LYP hybrid potential, reported for an 8-ZGNR (16 carbon atoms, $w \approx 16$ Å) a band-gap size of 1.34 eV,²⁷ compared to 1.02 eV from sX-LDA and 1.23 eV from G_0W_0 . So far, no experimental data exists for comparison of those calculated band-gap sizes with real values, however, the similar results from different nonlocal approaches suggests that the small values from LDA are indeed a severe underestimation of the real band-gap energies. There are two different factors for the size of the band gap. One is the quantum confinement, which induces an inversely proportional width-dependent band-gap energies, the other is the separation of the valence and the conduction band by formation of a spin-polarized ground state. To estimate the influence of the spins on the band-gap size, we fitted a function

$$E_g = \frac{A}{w + \Delta} \quad (2)$$

to the sX-LDA band-gap energies. Δ is the deviation length from the ideal quantum confinement law $E_g \propto \frac{1}{w}$ and is an indicator for the effect of the spin interaction. $\Delta = 9.3$ Å

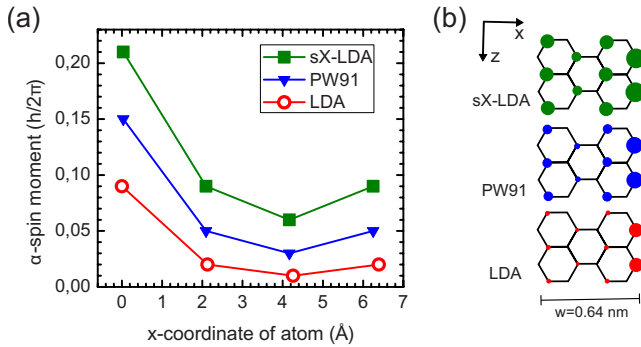


FIG. 3. (Color online) (a) Comparison of α spin momenta of a 4-ZGNR (eight atoms per unit cell) from calculations employing LDA (red circles). (b) Graphical representation of the spin momenta from (a) on the nanoribbon atoms. The ratio of the areas of the circles representing the spin momenta is the same as the ratio between the absolute values of the momenta.

gives good agreement with our calculated values. Yang *et al.* reported a value of $\Delta=16$ Å, which might imply a stronger contribution of the interaction of the electrons with the surrounding system in their G_0W_0 calculations.

We obtained the spin polarization of the electronic ground states of our investigated nanoribbons by optimization of the atomic positions and the electronic spins. Starting from a nonspin-polarized geometry, these optimizations resulted in antiferromagnetic ground states all our calculations within LDA, GGA-PW91, and sX-LDA. Figure 3(a) shows the momenta of the α -spin direction in case of a 4-ZGNR, a nanoribbon with eight carbon atoms per unit cell. The ground state from LDA calculations exhibits a comparatively weak spin polarization, which is strongly localized at the nanoribbon edges, see Fig. 3(b). The calculated spin momentum at the edges is $0.09\hbar$ and rapidly decreases to an almost negligible value of $0.01\hbar$ at the nanoribbon bulk atoms. This corresponds to a decrease of 88% over the distance of second-nearest neighbors. While the spin momenta from sX-LDA still show a noticeable localization at the edges, the spin polarization over the whole unit cell of the 4-ZGNR is more

balanced. The spin momentum at the edges is $0.21\hbar$, more than $2.5\times$ the value from LDA, and decreases by 71% into the nanoribbon bulk. As expected, GGA improves on the magnetic properties of the material. We found that the spin momenta from PW91 are quite in between the values from LDA and sX-LDA, falling from $0.15\hbar$ at the edges down to a value of $0.03\hbar$, i.e., a drop of about 80%. The same results hold for the momenta of the β spins but from the opposite edge and with negative values, and for wider nanoribbons. It is evident from the degree of spin polarization and the changed band-gap energies that the nonlocal component of the electron exchange indeed has a significant effect on the electronic properties of zigzag nanoribbons.

IV. CONCLUSION

In conclusion, we used the screened-exchange (sX-LDA) approximation to calculate the electronic band structure of graphene and zigzag graphene nanoribbons and compared the results with the band structures from LDA and the quasiparticle band structures from the G_0W_0 approach. The introduced electron-electron interaction in sX-LDA leads to a renormalization of the band structure and the Fermi velocity in the linear part of the π band in graphene, as was found in experiments and from G_0W_0 calculations. We report that the Fermi velocity from sX-LDA is comparable to the value from G_0W_0 calculations and in good agreement with experimental values. For zigzag nanoribbons, our calculations confirmed the significance of the nonlocal part of the electron exchange interaction for the degree of spin polarization and for the size of the spin-induced band gap in the electronic band structure. The nonlocal exchange results in a larger band gap compared with LDA and comparable to that from G_0W_0 . The spin momenta in the electronic ground state from sX-LDA calculations are noticeably higher and more balanced over the whole unit cell of graphene nanoribbons compared to results from LDA and GGA-PW91. As a result, we are confident that the screened-exchange-LDA approach is a useful alternative method for the study of electronic properties in graphene-related materials.

*rg403@cam.ac.uk

¹K. S. Novoselov, A. K. Geim, S. V. Morozov, D. Jiang, Y. Zhang, S. V. Dubonos, I. V. Grigorieva, and A. A. Firsov, *Science* **306**, 666 (2004).
²K. S. Novoselov, A. K. Geim, S. V. Morozov, D. Jiang, M. I. Katsnelson, I. V. Grigorieva, S. V. Dubonos, and A. A. Firsov, *Nature (London)* **438**, 197 (2005).
³A. Bostwick, T. Ohta, T. Seyller, K. Horn, and E. Rotenberg, *Nat. Phys.* **3**, 36 (2007).
⁴M. Sprinkle, D. Siegel, Y. Hu, J. Hicks, A. Tejada, A. Taleb-Ibrahimi, P. Le Fèvre, F. Bertran, S. Vizzini, H. Enriquez, S. Chiang, P. Soukiassian, C. Berger, W. A. de Heer, A. Lanzara, and E. H. Conrad, *Phys. Rev. Lett.* **103**, 226803 (2009).
⁵M. Orlita, C. Faugeras, P. Plochocka, P. Neugebauer, G. Martinez, D. K. Maude, A.-L. Barra, M. Sprinkle, C. Berger, W. A.

de Heer, and M. Potemski, *Phys. Rev. Lett.* **101**, 267601 (2008).
⁶Y. Zhang, Y.-W. Tan, H. L. Stormer, and P. Kim, *Nature (London)* **438**, 201 (2005).
⁷D. L. Miller, K. D. Kubista, G. M. Rutter, M. Ruan, W. A. de Heer, P. N. First, and J. A. Stroscio, *Science* **324**, 924 (2009).
⁸R. S. Deacon, K.-C. Chuang, R. J. Nicholas, K. S. Novoselov, and A. K. Geim, *Phys. Rev. B* **76**, 081406(R) (2007).
⁹Y.-W. Son, M. L. Cohen, and S. G. Louie, *Phys. Rev. Lett.* **97**, 216803 (2006).
¹⁰T. Miyake and S. Saito, *Phys. Rev. B* **68**, 155424 (2003).
¹¹P. E. Trevisanutto, C. Giorgetti, L. Reining, M. Ladisa, and V. Olevano, *Phys. Rev. Lett.* **101**, 226405 (2008).
¹²C. Attacalite and A. Rubio, *Phys. Status Solidi B* **246**, 2523 (2009).
¹³C.-H. Park, F. Giustino, C. D. Spataru, M. L. Cohen, and S. G.

- Louie, *Nano Lett.* **9**, 4234 (2009).
- ¹⁴D. M. Bylander and L. Kleinman, *Phys. Rev. B* **41**, 7868 (1990).
- ¹⁵A. Seidl, A. Görling, P. Vogl, J. A. Majewski, and M. Levy, *Phys. Rev. B* **53**, 3764 (1996).
- ¹⁶K. Xiong, J. Robertson, M. C. Gibson, and S. J. Clark, *Appl. Phys. Lett.* **87**, 183505 (2005).
- ¹⁷B. Lee and L. Wang, *J. Appl. Phys.* **100**, 093717 (2006).
- ¹⁸B. Lee and L. Wang, *Appl. Phys. Lett.* **87**, 262509 (2005).
- ¹⁹L. Yang, C.-H. Park, Y.-W. Son, M. L. Cohen, and S. G. Louie, *Phys. Rev. Lett.* **99**, 186801 (2007).
- ²⁰S. J. Clark, M. D. Segall, C. J. Pickard, P. J. Hasnip, M. I. J. Probert, K. Refson, and M. C. Payne, *Z. Kristallogr.* **220**, 567 (2005).
- ²¹L. Kleinman and D. M. Bylander, *Phys. Rev. Lett.* **48**, 1425 (1982).
- ²²H. J. Monkhorst and J. D. Pack, *Phys. Rev. B* **13**, 5188 (1976).
- ²³B. Lee, L.-W. Wang, C. D. Spataru, and S. G. Louie, *Phys. Rev. B* **76**, 245114 (2007).
- ²⁴M. Fujita, K. Wakabayashi, K. Nakada, and K. Kusakabe, *J. Phys. Soc. Jpn.* **65**, 1920 (1996).
- ²⁵M. Ezawa, *Phys. Rev. B* **73**, 045432 (2006).
- ²⁶L. Pisani, J. A. Chan, B. Montanari, and N. M. Harrison, *Phys. Rev. B* **75**, 064418 (2007).
- ²⁷E. Rudberg, P. Salek, and Y. Luo, *Nano Lett.* **7**, 2211 (2007).